Applied Catalysis B: Environmental 204 (2017) 107–118

Contents lists available at ScienceDirect

Applied Catalysis B: Environmental

journal homepage: www.elsevier.com/locate/apcatb

Research paper

Mixed $Ba_{1-x}La_xF_{2+x}$ fluoride materials as catalyst for the gas phase fluorination of 2-chloropyridine by HF

A. Astruc[a], S. Célérier[a,*], E. Pavon[b], A.-S. Mamede[b], L. Delevoye[b], S. Brunet[a]

[a] Institut de Chimie des Milieux et Matériaux de Poitiers (IC2MP), Université de Poitiers, faculté des sciences, bat B27, 4 rue Michel Brunet, CNRS, F-86073 Poitiers, France

[b] Univ. Lille, CNRS, ENSCL, Centrale Lille, Univ. Artois, UMR 8181, UCCS – Unité de Catalyse et Chimie du Solide, F-59000 Lille, France

ARTICLE INFO

Article history:
Received 23 September 2016
Received in revised form 7 November 2016
Accepted 10 November 2016
Available online 11 November 2016

Keywords:
Barium fluoride
Lanthanum fluoride
Mixed metal fluoride
Fluorination
2-fluoropyridine

ABSTRACT

The stability under different atmospheres (dry or wet nitrogen or air, HF, reaction medium) and the catalytic performances of BaF_2-LaF_3 based catalysts for the fluorination of 2-choropyridine by Cl/F exchange with HF as fluorinating agent were investigated. Thermal decomposition of metal trifluoroacetate and precipitation from nitrate precursor methods were used as synthesis methods. Depending on the synthesis method and the La/La + Ba molar ratio (x), an intimate mixture of BaF_2 and LaF_3 metal fluorides or a $Ba_{1-x}La_xF_{2+x}$ mixed metal fluoride with high specific surface area were formed. In comparison with BaF_2, the mixed metal fluorides led to higher specific surface areas and prevented the sintering phenomenon observed under wet atmosphere which led to a significant decrease of the specific surface area. Moreover, $Ba_{1-x}La_xF_{2+x}$ catalysts had not evolved under the fluorination reaction contrary to BaF_2 for which a stable $BaF_{2-x}Cl_x$ material (with x close to 0.8) was formed by reaction with the by-product HCl. The turn over frequency (TOF) was similar for all barium based catalysts for the fluorination of 2-chloropyridine. Nevertheless, among the studied materials, $Ba_{0.5}La_{0.5}F_{2.5}$ was the most promising catalyst for the transformation of 2-chloropyridine due to high activity (related to its high specific surface area and its moderate strength of Lewis acidity) and high stability.

1. Introduction

Few applications with BaF_2 as catalyst were reported in the literature, the main are dehalogenation [1], oxidative hydrogenation of ethane (ODE) [2,3], oxidative coupling of methane (OCM) [4,5] and Cl/F exchange reactions [6]. BaF_2 was the most selective dehydrochlorination catalyst of 3-chloro-1,1,1,3-tetrafluorobutane due to its weak strength of Lewis acidity unlike AlF_3 which was highly selective for dehydrofluorination (higher Lewis acidity, greater affinity towards fluorine than chlorine) [1]. The addition of BaF_2 to several rare earth oxides or oxyfluorides substantially improved the catalytic properties and more specifically the selectivity for ODE and OCM reactions [2–5]. The presence of BaF_2 increased the number of anionic vacancies and defects (by ionic substitutions between Ba^{2+} and Me^{3+} and between F^- and O^{2-}) and the numbers of O_2^{2-} and O^- species allowing improvement of the catalytic performances. Nevertheless, these ODE and OCM experiments were carried out at high temperatures (800–1000 °C) and, the specific surface areas of these catalysts were very low (<10 $m^2\,g^{-1}$). BaF_2 was the most active catalyst compared to a series of metal fluorides (CaF_2, MgF_2, ZnF_2, LaF_3 and CeF_3) for the transformation of 2-chloropyridine into 2-fluoropyridine used as fluorinated building blocks for agrochemicals and pharmaceuticals applications [6]. These results were explained by a lower acid strength of the active sites. Indeed, chloropyridine compounds which were adsorbed on coordinately unsaturated site of the metal (Lewis acid sites) by the nitrogen atom, acted as poison of the sites if the strength of Lewis acidity is too high. Moreover, this catalyst exhibited a different behavior from other materials since the formation of a barium mixed halides ($BaCl_xF_{1-x}$) has been highlighted by reaction with HCl, the by-product of the reaction [1,6]. This solvent-free and very selective (100%) reaction to produce fluorinated pyridine compounds is promising taking account of the environmental regulations [7,8].

Mixed barium – lanthanum based systems ($Ba_{1-x}La_xF_{2+x}$) were reported in the literature mainly for electrochemical devices [9–12] involving the good fluorine conductivity or for up/down-conversion luminescence, laser devices or optical fibers applications [13–15]. No catalytic applications were reported. These materials were mainly prepared by solid state synthesis

* Corresponding author.
E-mail address: stephane.celerier@univ-poitiers.fr (S. Célérier).

http://dx.doi.org/10.1016/j.apcatb.2016.11.019
0926-3373/

[9,16], leading to the formation of large particles and probably low specific surface area. Mechanosynthesis [10,11] was also reported leading to the formation of small crystallites (10–30 nm). Some soft chemistry synthesis such as hydrothermal [14] or solvothermal synthesis [15] were also described without data of the specific surface areas. The preparation of these materials by thermal decomposition of metal trifluoroacetate or by co-precipitation were only reported for the nominal composition $Ba_{0.57}La_{0.43}F_{2.43}$ obtained by co-precipitation [17]. As described by the phase diagram proposed by Sobolev et al. [16], $Ba_{1-x}La_xF_{2+x}$ crystallizes in a fluorite structure (space group *Fm*-3m) for x compositions lower than 0.55 and in a tysonite structure (space group *P*-3*c*1) for x compositions higher than 0.85. In the intermediate x compositions (from 0.55 to 0.85), a mixture of mixed metal fluorides were noticed. Nevertheless, in this range, Duvel et al. [11] synthesized successfully a pure $Ba_{1-x}La_xF_{2+x}$ mixed metal fluoride with the fluorite structure by mechanosynthesis.

The aim of this work is to investigate and to understand the change of barium-lanthanum fluoride based systems at each step of their preparation, storage and for the transformation of 2-chloropyridine. More specifically, the impact of the atmosphere of storage (dry or wet nitrogen or air), the evolution during the HF activation step and the transformation of the chlorinated substrate were studied. The Ba-La fluoride based materials were prepared by thermal decomposition of metal trifluoroacetates and by precipitation methods. All of the various solids were characterized in order to determine the composition, the morphology, the structure, the specific surface area and the Lewis acidity (amount and strength) of the active sites. Finally, the performances (in term of activity and stability) of these solids were compared for the transformation of 2-chloropyridine used as model molecule for catalytic Cl/F exchanges and correlated with their properties.

2. Experimental

2.1. Catalyst preparations

BaF_2, LaF_3 and mixed $Ba_{1-x}La_xF_{2+x}$ ($0 < x < 1$) fluorides catalysts were prepared by thermal decomposition of the corresponding trifluoroacetates and by precipitation from the corresponding nitrates.

2.1.1. BaF_2 samples

BaF_2 was obtained by thermal decomposition of barium trifluoroacetate ($Ba(CF_3COO)_2$) at 350 °C under nitrogen for 4 h [6]. $Ba(CF_3COO)_2$ was synthesized from $Ba(CH_3COO)_2$ (Sigma-Aldrich, 99%) and trifluoroacetic acid (TFA) (Sigma-Aldrich, 99%) in acetic acid (Sigma-Aldrich, 99.7%) which acted as solvent. The TFA/Ba molar ratio was equal to 9 and the amount of the solvent was adjusted to obtain a barium concentration of 0.5 mol L^{-1}. The solution was then dried at 160 °C during 12 h before the decomposition step.

To study the influence of the storage conditions, BaF_2 samples were stored in different conditions listed in Table 1 with their corresponding names.

2.1.2. Mixed barium-lanthanum fluorides

Bimetallic fluorides ($Ba_{1-x}La_xF_{2+x}$ with $x = La/(La + Ba)$ molar ratio ranging from 0 to 1) were synthesis by thermal decomposition of metal trifluoroacetates (TDT) and by precipitation (P).

By TDT method, 5x mmol of $La(CH_3COO)_2,6H_2O$ (Sigma-Aldrich, 99.9%) and $5(1-x)$ mmol of $Ba(CH_3COO)_2$ (Sigma-Aldrich, 99%) were introduced with the adjusted amount of acetic acid (Sigma-Aldrich, 99.7%) to obtain a concentration of metals (La + Ba) of 0.5 mol L^{-1}. Then, 45 mmol of trifluoroacetic acid were added to form a bi-metallic trifluoroacetate or a homogeneous mixture of monometallic trifluoroacetates. As an example, for a molar ratio (x) of 0.2, 0.316 g of $La(CH_3COO)_2$, $6H_2O$ and 1.02 g of $Ba(CH_3COO)_2$ were added to 100 mL of acetic acid following by the addition of 3.4 mL of trifluoroacetic acid. The solution of metal trifluoroacetates was then dried at 160 °C during 12 h and decomposed at 350 °C under nitrogen for 4 h.

By the precipitation (P) method, 5x mmol of $La(NO_3)_2,6H_2O$ (Sigma-Aldrich, 99%) and $5(1-x)$ mmol of $Ba(NO_3)_2$ (Sigma-Aldrich, 99%) were dissolved in deionized water to obtain a concentration of metals (La + Ba) of 0.1 mol L^{-1}. Then, this solution was introduced drop by drop into a HF solution of 10 mol L^{-1} to obtain a HF/metal molar ratio of 100. As an example, for a molar ratio (x) of 0.2, 0.43 g of $La(NO_3)_2,6H_2O$ and 1.05 g of $Ba(NO_3)_2$ previously dissolved into 50 mL of water were added into 50 mL of aqueous HF of 10 mol L^{-1}. The white precipitates were filtered and washed several times with deionized water before drying at 100 °C during 12 h.

The various samples prepared by the 2 methods were then stored in a glove box under dry nitrogen.

2.2. Characterizations

The specific surface area, the composition, the structure, the morphology and the Lewis acid properties were measured before and after the 2-chloropyridine transformation by nitrogen physisorption, elemental analysis, thermal analysis, X-Ray diffraction, transmission electronic microscopy, ^{19}F solid-state NMR, XPS and CO adsorption followed by Infra-Red.

Nitrogen adsorption-desorption was performed at −196 °C using a TRISTAR 3000 gas adsorption system. Prior to N_2 adsorption, the powder samples were degassed under vacuum for 2 h at 250 °C (or 80 °C for materials prepared at 100 °C). The moisture sensitive samples were prepared in a N_2 glove box before treatment under vacuum. The BET equation was used to calculate the surface area (S_{BET} in $m^2\,g^{-1}$) of the samples at relative pressures between 0.05 and 0.30. Considering spherical particles with only inter-particles porosity, the average particle size (d_{BET}) of BaF_2 samples were calculated: $d_{BET}=6/(\rho.S_{BET})6/(\rho\cdot S_{BET})$ with ρ the volumetric mass density ($_{\rho BaF2}$ = 4.893 g cm^{-3}).

Barium contents were determined by inductively coupled plasma-optical emission spectrometry (ICP-OES) using a PerkinElmer Optima 2000DV instrument and F content with ion chromatography (DIONEX ICS-2000).

Thermogravimetric analyses (TGA) and differential thermal analyses (DTA) were performed using Q600 TA Instrument apparatus coupled with a mass spectrometer (MS) (QGA-Hiden Analytical) under dry air (5 °C min^{-1} from room temperature to 700 °C with an isotherm of 90 min at room temperature) in order to investigate the thermal behavior of different BaF_2 samples. For mass spectrometry, *m*/*z* from 1 to 100 were analyzed.

XRD analyses of samples were carried out on a PANalytical EMPYREAN powder diffractometer using CuK_α radiation source ($K_{\alpha1}$ = 1.5406 Å and $K_{\alpha2}$ = 1.5444 Å) in order to reveal the crystallographic structure of each sample. These patterns were collected with a 0.033° step and 120 s dwell time at each step between 20 and 140°. Phase identification was performed by comparison with the ICDD database reference files. Cell parameters were determined from Rietveld refinements using Highscore software. The x content of the synthesized $Ba_{1-x}La_xF_{2+x}$ was determined using the Vegard's law with the equations proposed by Chable et al. [9] for the tysonite structure ($a = a_0 + 0.3855(1-x)$ and $c = c_0 + 0.4460(1-x)$) and Sobolev et al. [16] for the fluorite structure ($a = a_0' - 0.3033x$) (with a and c, the cell parameters of the $Ba_{1-x}La_xF_{2+x}$ solid solution, a_0 and c_0 the cell parameters of LaF_3 and a_0' the cell parameter of BaF_2). The moisture sensitive samples were prepared in a glove box and covered during the analysis with a Kapton foil.

Table 1
Storage conditions of BaF_2 samples.

Samples	Storage
BaF_2	Glove box with dry nitrogen
BaF_2-air-xd	Ambient air with different duration of exposure (x = 1 or 30 days)
BaF_2-wet-N_2	Wet nitrogen (powder exposed to a stream of N_2 bubbling in water during one day)
BaF_2-wet-air	Wet air (powder exposed to a stream of air bubbling in water during one day)

Transmission Electronic Microscopy (TEM) were carried out using a JEOL 2100 instrument (operated at 200 kV with a LaB_6 source and equipped with a Gatan Ultra scan camera).

XPS analysis were performed using a Kratos Analytical AXIS Ultra^{DLD} spectrometer. A monochromatic aluminum source (Al Kα = 1486.6 eV) was used for excitation. The analyser was operated in constant pass energy of 40 eV using an analysis area of approximately 700 μm × 300 μm. Charge compensation was applied to compensate for the charging effect occurring during the analysis. The adventitious C 1s (285.0 eV) binding energy (BE) was used as internal reference. Quantification of the experimental photopeaks were carried out using CasaXPS software.

The ^{19}F solid-state NMR spectra were acquired on a Bruker Avance III 800 spectrometer operating at 752.86 MHz for ^{19}F using a 1.3 mm (outer rotor diameter) probehead. The spinning frequency was 60 kHz, the recycle delay was 10 s and 64 scans were collected using a 90° pulse excitation of 2.25 μs. ^{19}F chemical shifts were given in ppm with respect to solid CaF_2 used as secondary reference set to −108 ppm.

CO adsorption followed by FTIR spectroscopy was carried out using a ThermoNicolet NEXUS 5700 spectrometer with a resolution of 2 cm^{-1} and 64 scans per spectrum were collected. Samples were pressed into thin pellets (10–60 mg) with diameter of 16 mm and activited *in situ* during one night at 350 °C under high vacuum (≈10^{-6} bar). After cooling down the samples to room temperature, the cell was cooled down with liquid nitrogen to 100 K. A background spectrum was collected which was then subtracted to the other spectra obtained after CO adsorption. Then, successive doses of CO were introduced quantitatively and an infrared spectrum was recorded after each adsorption until saturation. The final spectrum was recorded with 1 Torr of CO at equilibrium pressure (saturation). All spectra were normalized to an equivalent sample mass (25 mg). The quantification of the amount of Lewis acid sites Q_s (mmol g^{-1}) was carried out by the integration of the total area of the IR bands at saturation between 2100 and 2200 cm^{-1} using the molar absorption coefficient ε of each material. To determine ε, a linear variation was obtained up to a plateau corresponding to the saturation of surface sites by plotting the overall intensity of the ν(CO) band versus the amount of CO introduced, ε corresponding to the slope of the straight line. Note that due to the possibility of the formation of dicarbonyl species at high coverage [18] an overestimated value of the coordinatively unsaturated sites (CUS) (Lewis acid sites) was probably measured in each case.

2.3. Reaction conditions

As described previously [6], catalytic activity measurements for the transformation of 2-chloropyridine were carried out in a fixed-bed reactor at 300 °C at atmospheric pressure during 4 h 30. The different barium fluoride based catalysts were diluted with 6 cm^3 of Lonza graphite (size grains between 125 and 200 μm). For specific experiments, the reaction time varied from 1 h to 9 h. Firstly, the catalyst was activated *in situ* by HF under nitrogen (N_2/HF: 1/4) for 1 h at 350 °C (activation step). Then, 2-chloropyridine was introduced into the reactor using a syringe pump. The partial pressures of the various components were 0.806 bar for HF, 0.075 bar for 2-chloropyridine and 0.132 bar for nitrogen (HF/2ClPy/N_2: 10.8/1/1.7). The organic gas products were trapped into 1,2-dichloroethane. HF and HCl were quenched in water at the outlet of the reactor. The organic components were analyzed with a Scion 456 gas-phase chromatograph (Bruker) equipped with a DB5 capillary column (inside diameter: 0.2 mm; thickness film: 1 μm, length: 30m). The oven temperature was raised from 100 to 200 °C at a rate of 5 °C min^{-1}.

Table 2
Specific surface areas (S_{BET}) before and after the activation step by HF (T = 350 °C, one hour), and sizes of particles determined from S_{BET} and XRD of various samples of BaF_2.

Samples	S_{BET}		d_{BET}[a]	d_{XRD}[b]
	Before activation by HF	After activation by HF		
BaF_2	63	47	19	19
BaF_2-air-1d	47	42	26	27
BaF_2-air-30d	36	35	34	35
BaF_2-wetN_2	25	27	48	48
BaF_2-wetair	22	24	56	59

[a] Size of particles calculated from S_{BET} before activation by HF.
[b] Size of crystallites calculated with the Debye-Scherrer equation applied to the (111) reflection at 2θ = 24.85° before activation by HF.

The catalyst performances were compared at a conversion of 2-chloropyridine lower than 25% in order to be in a differential regime. The catalytic activity A (mmol h^{-1} g^{-1}) was defined as the conversion of 2-chloropyridine multiplied by the flow of the chlorinated substrate (mol h^{-1}) and divided by the mass of catalyst. The intrinsic catalytic activity A_i (mmol h^{-1} m^{-2}) was calculated taking into account the specific surface area of the catalyst after the activation step by HF. In all case, only 2-fluoropyridine (2FPy) was observed as reaction product and HCl as by-product. Thus, the selectivity towards 2-fluoropyridine was equal to 100% and the conversion of 2-chloropyridine corresponded to the 2-fluoropyridine yield. In these experiments, the molar balance was always higher than 90%. No thermal decomposition of 2-chloropyridine was observed.

The Turn Over Frequency TOF (h^{-1}) was calculated from the catalytic activity (A: mmol h^{-1} g^{-1}) divided by the amount of actives sites defined as coordinatively unsaturated metallic sites (Q_s :mmol g^{-1}) measured by CO adsorption followed by IR.

3. Results

3.1. Effect of the storage atmosphere on the stability of BaF_2 based catalysts

The influence of the atmosphere (air and nitrogen, dry and wet) of storage of various BaF_2 samples on their specific surface area (S_{BET}) and their particles sizes (d) (determined from BET and XRD datas) are reported in Table 2. As previously described [6], crystallized BaF_2 (cubic, *Fm*-3m) was obtained by thermal decomposition of barium trifluoroacetate at 350 °C under nitrogen during 4 h without formation of secondary phase (Fig. 1a). When this material was stored in a glove box under dry nitrogen, the specific surface area was equal to 63 m^2 g^{-1} whatever the duration of storage. However, a significant decrease to 47 m^2 g^{-1} and to 36 m^2 g^{-1} was observed after respectively one-day exposure to ambient air (BaF_2-air-1d)

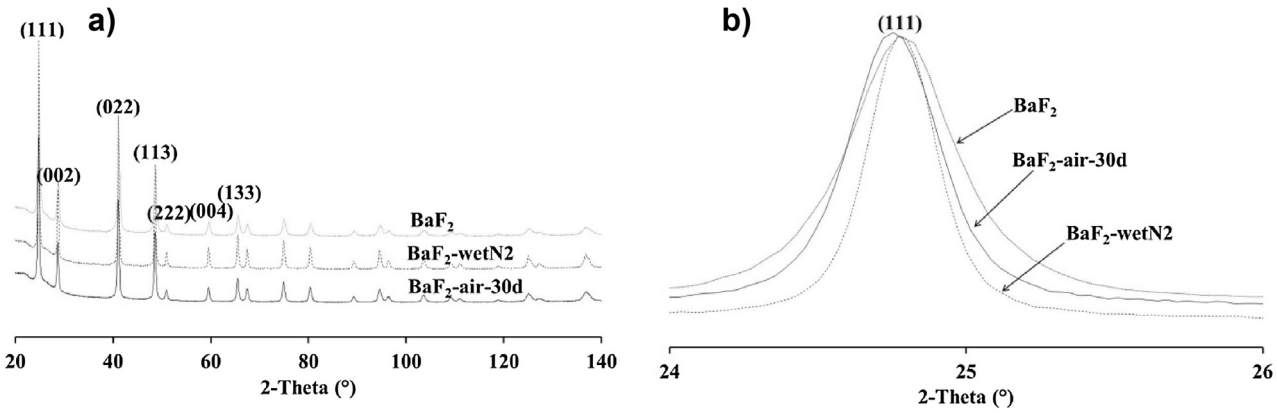

Fig. 1. Effect of the atmosphere of storage of BaF_2 samples (BaF_2, BaF_2-wetN_2, BaF_2-air-30d) a) X-Ray diffraction patterns (in brackets: main *hkl* indices of the BaF_2 structure, Fm–3m space group). b) (111) diffraction peaks of BaF_2 samples normalized to the same intensity.

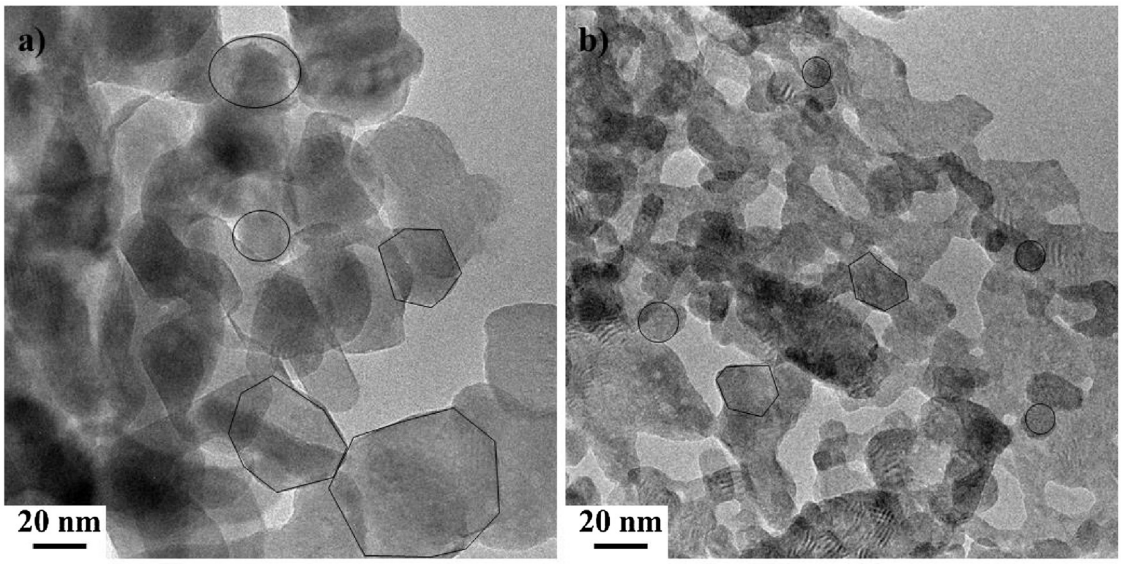

Fig. 2. TEM analysis of : a) BaF_2-wetN_2 and b) BaF_2.

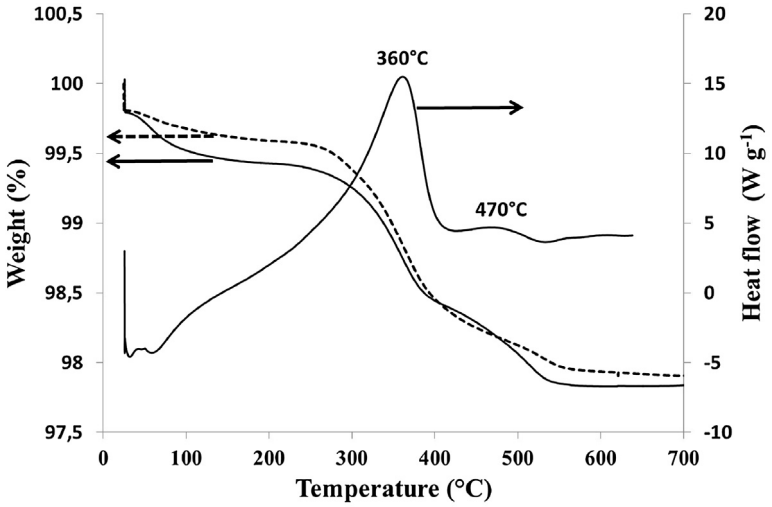

Fig. 3. TGA and DTA curves of BaF_2 (solid line) and TGA curve of BaF_2-wetN_2 (dotted line).

and after 30-days (BaF_2-air-30d). As a further step, an exposure of BaF_2 to atmosphere saturated with water (nitrogen and air) during one-day led to a reduced specific surface area of 20–25 $m^2\ g^{-1}$. This corresponded to an increase of the crystallite sizes, determined from XRD (decrease of the full width at half maximum of the most intense peak of BaF_2 structure: Fig. 1b) from 19 nm for BaF_2 to 59 nm for BaF_2-wetair (Table 2). This was confirmed by the determination of the size of particles from the specific surface area (d_{BET}) (Table 2) and by TEM analysis of BaF_2 samples (respectively Fig. 2b for BaF_2 stored in a glove box and Fig. 2a for BaF_2 stored under wet nitrogen). Indeed, particles with diameters between 15 and 25 nm for BaF_2 (some particles are surrounded for clarity) and between 30 and 60 nm for BaF_2-wetN_2 were noticed. This modification of the specific area did not correspond to a change of crystal structure since the diffraction peaks were similar (Fig. 1a). On the other hand, BaF_2 and BaF_2-wetN_2 samples were analyzed and compared by thermal analyses coupled with mass spectrometry (Fig. 3). During the isotherm at room temperature, a small weight loss (less than 0.2% for each sample) was observed with BaF_2 (stored in a glove box under dry nitrogen) and BaF_2-wetN_2 samples. Below 100 °C, the weight loss continued until 0.5% for BaF_2 and 0.4% for BaF_2-wetN_2 corresponding to the elimination of physisorbed water as confirmed by mass spectrometry (peak of $m/z = 18$, not shown). This endothermic phenomena was confirmed by DTA curve with negative peaks below 100 °C. This result indicated that no more water was adsorbed on the sample stored under wet atmosphere. Two weight losses were observed at 360 °C and 470 °C as indicated by exothermic DTA peaks, both corresponding to the formation mainly of CO_2 gas ($m/z = 44$) with traces of H_2O ($m/z = 18$) due to oxidation of the carbon-bearing impurities formed during thermal decomposition of barium trifluoroacetate [6,19,20]. After treatment at 700 °C, XRD analyses of both materials confirmed that no pyrohydrolysis phenomenon was involved since the cubic structure of BaF_2 was retained. Finally, no significant difference of thermal behavior between both BaF_2 samples were observed which confirmed that the structure and the composition of BaF_2 was retained after exposure under wet atmosphere. This is in accordance with the elemental analyses which did not reveal changes. The Ba/F molar ratio was close to 2 for the different BaF_2 samples whatever the storage conditions.

Under HF gas (corresponding to the activation step: 350 °C, one hour) before the transformation of 2-chloropyridine, only the specific surface area of BaF_2 decreased from 63 $m^2\ g^{-1}$ to 47 $m^2\ g^{-1}$ without structural modification (Table 2). No significant change of the specific surface area for the other samples was observed. This decrease of the specific surface area was probably due to the unavoidable contact with air of the BaF_2 powder, previously stored in a glove box, before and after transfer in the reactor for the activation step. This drop of the specific surface area of BaF_2 was independent of the duration of this activation step since the surface remained close to 47 $m^2\ g^{-1}$ between 30 min and 4 h.

3.2. Synthesis and characterization of mixed Ba-La fluoride systems

Various mixed Ba-La samples with La/(La + Ba) molar ratio (x) ranging from 0 to 1 were synthesized by thermal decomposition of the corresponding trifluoroacetates (TDT) and by precipitation from nitrate precursors (P). XRD characterizations were reported respectively Fig. 4 for TDT and Fig. 5 for P methods.

As expected, the monometallic fluorides (x = 0 for BaF_2 and x = 1 for LaF_3) were obtained from both methods (TDT and precipitation) without formation of secondary phase (Fig. 4 and 5). Whatever the method, BaF_2 with the cubic fluorite type structure and LaF_3 with the trigonal tysonite type structure were obtained. The cell parameters obtained by Rietveld refinements (Table 3) on these solids

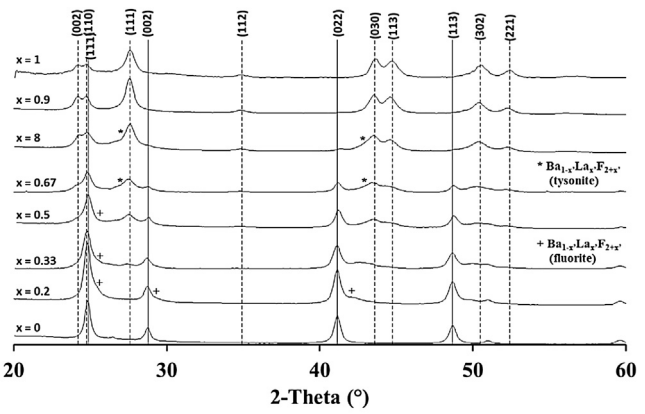

Fig. 4. XRD patterns of the Ba-La fluoride systems prepared by TDT method as a function of La/(La + Ba) molar ratio (x). In brackets: main *hkl* indices of BaF_2 (solid line) and LaF_3 (dotted line).

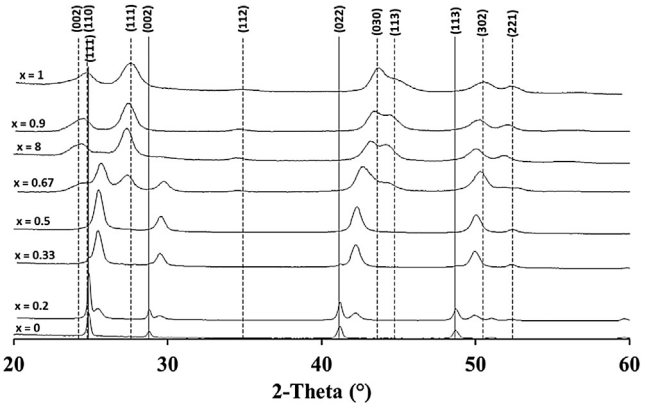

Fig. 5. XRD patterns of the Ba-La fluoride systems prepared by precipitation method as function of La/(La + Ba) (x) molar ratios. In brackets: main *hkl* indices of BaF_2 (solid line) and LaF_3 (dotted line).

Table 3
Cell parameters and composition (x') of the $Ba_{1-x}La_xF_{2+x}$ mixed fluoride prepared by precipitation method according to initial x.

x = La/La + Ba	Structure[a]	a (Å)	c (Å)	x'[d]
0	c		6.1997 (5)	0
0.2[b]	c		6.0548 (3)	0.48
0.33[b]	c		6.0530 (9)	0.48
0.5	c		6.0436 (6)	0.51
0.67	c		6.0142 (9)	0.61
	q	7.253 (2)	7.256 (1)	0.84
0.8[c]	q	7.433 (3)	7.437 (2)	0.83
0.9	q	7.227 (2)	7.406 (2)	0.90
1	q	7.188 (2)	7.363 (3)	1

[a] c: cubic fluorite type structure, q: trigonal tysonite type structure.
[b] Have also BaF_2 in the sample.
[c] Have also a minority mixed cubic phase.
[d] x' content determined from Vegard's law [9,16].

obtained by precipitation method corresponds to those reported in the literature [9,16]. For TDT, regarding the intermediates corresponding to $0.2 < x < 0.9$, a mixture of BaF_2 (illustrated by the 022 reflection peak which intensities decrease with x) and LaF_3 (illustrated by the 030 and 113 reflection peaks which intensities increase with x) was mainly formed. Nevertheless, for $0.2 \leq x \leq 0.8$, some shoulders were observed corresponding to the presence of a mixed $Ba_{1-x'}La_{x'}F_{2+x'}$ phase, in low amount, with a cubic ($0.2 \leq x \leq 0.5$) or trigonal ($0.67 \leq x \leq 0.8$) structure. In this case, the determination of the cell parameters of these mixed phases was difficult since the diffraction peaks had a low intensity and were often

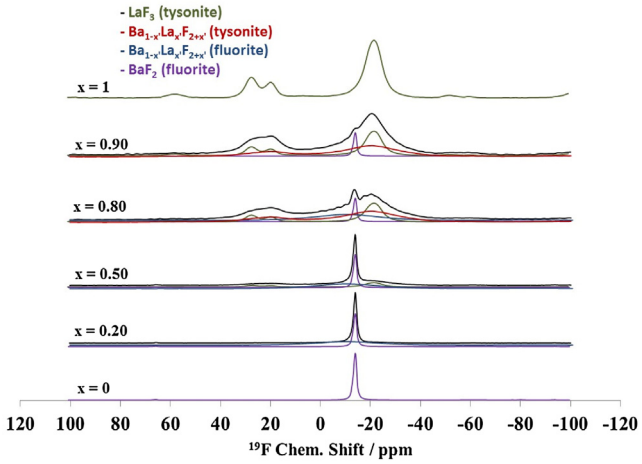

Fig. 6. ^{19}F MAS NMR spectra of Ba-La fluoride systems synthesized by TDT as a function of La/(La + Ba) molar ratio (x) together with the different contributions obtained by best-fit simulations for $0.2 \leq x \leq 0.9$. (in colour).

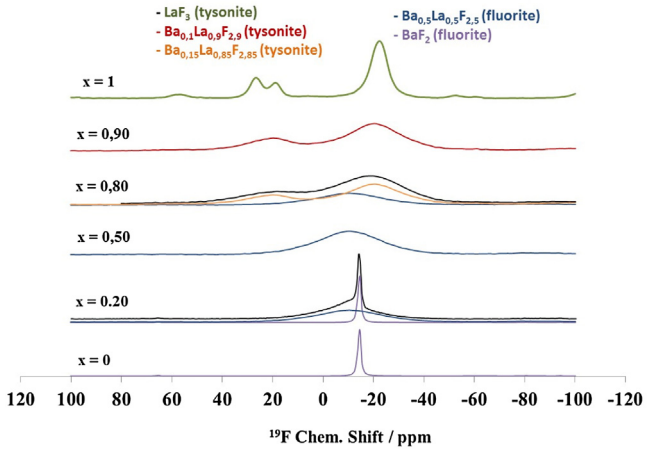

Fig. 7. ^{19}F MAS NMR spectra of Ba-La fluoride systems synthesized by precipitation method (P) as a function of La/(La + Ba) molar ratio (x) together with the different contributions obtained by best-fit simulations for $0.2 \leq x \leq 0.8$. (in colour).

confused with the monometallic phases. ^{19}F MAS NMR analysis of the various samples obtained by TDT is showed Fig. 6. For x = 0, a resonance at −14.9 ppm was observed which is close to the chemical shift of BaF_2 described in the literature (−14.3 ppm, [21]). For x = 1, the spectrum can be fitted with 3 resonances (−22.3, 19.1 and 26.4) assigned to 3 fluorine crystallographic sites of LaF_3 as described in ref [9], named F_1, F_2 and F_3 respectively. For the intermediate values of x, the mixture of the monometallic fluorides was confirmed by the deconvolution of the spectrum with the different contributions corresponding to BaF_2 and LaF_3 except for x = 0.2 (Fig. 6). Nevertheless, some other contributions with different shifts associated to a fluorite or tysonite phase were observed and showed the formation of minority mixed phases. For x = 0.8, two mixed fluorides were proposed by deconvolution whereas only the tysonite mixed phase was observed by XRD (Fig. 4). Thus, it seems that this method was not well adapted to obtain pure mixed phases probably due to the formation of a mixture of monometallic trifluoroacetates instead of a bimetallic trifluoroacetate before the thermal decomposition. Nevertheless, the presence of minority mixed phases suggested the formation of an intimate mixture of metal fluorides.

On the other hand, crystallized phases obtained by precipitation method were totally different for $0.2 \leq x \leq 0.9$ in comparison with TDT method. Indeed, a mixture of a cubic mixed phase and BaF_2 was observed for $0.2 \leq x \leq 0.33$ (Fig. 5). The amount of this mixed phase increased with the La/(La + Ba) molar ratio (x). The cell parameters of this cubic mixed phase was determined (Table 3) corresponding to a composition of $Ba_{0.48}La_{0.52}F_{2.54}$ considering the Vegard's law [16]. For x = 0.5, pure $Ba_{0.51}La_{0.49}F_{2.48}$ mixed phase was obtained with a composition very close to the initial La/(La + Ba) molar ratio introduced for the synthesis. For $0.6\,7 \leq x \leq 0.8$, a mixture of a cubic mixed phase and a trigonal mixed phase with an approximate composition of $Ba_{0.16}La_{0.84}F_{2.84}$ was observed (x′ = 0.84 for initial x = 0.67 and x′ = 0.83 for initial x = 0.8). The composition of the cubic phase with x = 0.67 was $Ba_{0.39}La_{0.61}F_{2.61}$ (Table 3). The cell parameters and the chemical composition for x = 0.8 of the cubic phase were not determined due to the very low intensity of the corresponding reflection peaks. Finally, for x = 0.9, the mixed phase $Ba_{0.1}La_{0.9}F_{2.9}$ with x′ corresponding to the initial content x was obtained. The ^{19}F MAS NMR analyses confirmed the XRD results (Fig. 7). The resonance F_1 at −22.3 ppm for LaF_3 (x = 1) shifted to −20.4 ppm for x = 0.9 and −19.1 ppm for x = 0.8 and corresponded to the substitution of the lanthanum by the barium in the tysonite structure [9]. Moreover, for x = 0.8, a second contribution was required in the best fit simulation corresponding to a cubic phase with a shift at −10.7 ppm. It could be assigned to $Ba_{0.5}La_{0.5}F_{2.5}$. Indeed, for x = 0.5, where only the phase $Ba_{0.5}La_{0.5}F_{2.5}$ was reported by XRD, a shift at −10.7 ppm was observed. This shift was also obtained by deconvolution of the spectrum for x = 0.2 in accordance with the XRD results. The shift corresponding to BaF_2 was also observed on this sample. Contrary to TDT method, the synthesis by precipitation method led to the formation of pure mixed phases: $Ba_{0.5}La_{0.5}F_{2.5}$ with a cubic fluorite structure and $Ba_{0.1}La_{0.9}F_{2.9}$ with a trigonal tysonite structure. The size of the crystallites for the samples obtained by precipitation method, determined by Debye-Scherrer equation, were very small respectively between 8 and 14 nm for the mixed fluoride with fluorite structure and between 5 and 8 nm for the mixed fluoride with tysonite structure.

The specific surface area of the various samples synthesized by the two methods corresponding to $Ba_{1-x}La_xF_{2+x}$ mixed fluorides or a mixture of monometallic fluorides were determined (Table 4). From TDT, the specific surface area varied from 84 to 98 $m^2\,g^{-1}$ with $0.2 \leq x \leq 0.9$, corresponding to a mixture of monometallic fluorides, which was significantly higher than the surface obtained for BaF_2 (63 $m^2\,g^{-1}$) and LaF_3 (81 $m^2\,g^{-1}$). This soft chemistry synthesis involved the formation of an intimate mixture of Ba and La precursors which could reduce the crystallization and the growth of the particles of the monometallic fluorides leading to higher specific surface areas. By precipitation method, the specific surface areas were relatively high except for BaF_2 (< 3 $m^2\,g^{-1}$) and varied from 33 to 132 $m^2\,g^{-1}$ by increasing the lanthanum content (x). The low specific surface area of BaF_2 comes from the presence of water as solvent of the synthesis. Indeed, as explained previously, water is in favor of the decrease of the specific surface area of BaF_2. Thus, whereas this method was well adapted to obtain mixed fluorides in comparison with TDT, the precipitation under these conditions was not adapted to synthesize BaF_2 with significant specific surface area.

Regarding the stability of the structural and microstructural properties of these materials under wet air, no structural modification was observed by XRD whatever the synthesis method and La/(La + Ba) molar ratios. As expected since the synthesis was led in water, no modification of the specific surface area was observed for the samples prepared by precipitation method after exposition under wet air (Table 4). In contrast, the specific surface area of the samples prepared by TDT decreased after exposition. This is due to the presence of BaF_2 in these samples which is sensitive to wet atmosphere. Nevertheless, the decrease of the surface was lower in the presence of lanthanum. Indeed, the specific surface areas of the samples for $0.2 \leq x \leq 0.9$ varied from 52 to 66 $m^2\,g^{-1}$ after exposi-

Table 4
Specific surface area (S_{BET}: $m^2\ g^{-1}$) of the Ba-La fluorides system prepared by TDT (thermal decomposition of metal trifluoroacetates) and precipitation methods as a function of x (La/(La + Ba) molar ratio) stored under inert atmosphere (N_2: glove box), wet air at room temperature and after activation by HF (T = 350 °C, 1 h, HF = 0.23 mol h^{-1}).

x	TDT			Precipitation		
	dry N2	wet air[a]	after activation by HF	dry N2	wet air[a]	after activation by HF
0	63	22	47	< 3	< 3	< 3
0.2	85	52	63	33	33	30
0.33	84	48	65	53	52	41
0.5	98	57	73	58	58	38
0.67	89	62	71	82	82	47
0.8	96	63	72	88	87	45
0.9	89	66	75	96	101	42
1	81	79	75	132	119	25

[a] Powder exposed to a stream of air bubbled through water during 24 h at room temperature.

tion in comparison with 22 $m^2\ g^{-1}$ for x = 0. These higher specific surface areas could be explained by the higher initial specific surface areas of the mixture and the presence of lanthanum fluoride which limited the growth of the barium fluoride particles. Thus, the presence of lanthanum allowed to retain substantially the high specific surface areas of the catalysts under wet atmosphere and stabilized their microstructural properties, particularly when the precipitation method was used. Interestingly, a low amount of lanthanum (x = 0.2) was sufficient to increase drastically the specific surface areas, even after exposition under wet air, in comparison with BaF_2 (22 $m^2\ g^{-1}$) whatever the synthesis method (52 $m^2\ g^{-1}$ by TDT and 33 $m^2\ g^{-1}$ by precipitation).

After activation under HF, a decrease of the specific surface area was also observed regardless of x content for Ba-La fluorides system prepared by TDT method (Table 4). Nevertheless, higher specific surface areas were retained with $0.2 \leq x \leq 1$ (from 63 to 75 $m^2\ g^{-1}$) in comparison with BaF_2 (47 $m^2\ g^{-1}$). Regarding the samples prepared by precipitation method, the decrease of the surface was more important, particularly when the lanthanum amount increased. This drop of the surface was mainly the result of the thermal activation of the sample at a temperature (350 °C) higher than the temperature of preparation (100 °C). Nevertheless, except for BaF_2, significant specific surface areas were retained from samples prepared by precipitation method (30 to 47 $m^2\ g^{-1}$). Interestingly, the synthesis of pure mixed metal fluorides (x = 0.5 and 0.9) by this method allowed to obtain higher specific surface areas after activation under HF (38 $m^2\ g^{-1}$ for $Ba_{0.5}La_{0.5}F_{2.5}$ and 42 $m^2\ g^{-1}$ $Ba_{0.1}La_{0.9}F_{2.9}$) than the corresponding monometallic fluorides prepared in the same way (< 3 $m^2\ g^{-1}$ for BaF_2 and 25 $m^2\ g^{-1}$ for LaF_3) highlighting a synergetic effect between barium and lanthanum on the microstructural properties.

3.3. Characterization of the Lewis acidity of Ba-La based catalysts by CO adsorption followed by FTIR

The storage of BaF_2 catalyst under wet atmosphere did not modify the strength of Lewis acidity. Indeed, the same four bands of ν(CO) (2167, 2158, 2152 and 2146 cm^{-1}) were observed (Fig. 8) whatever the storage conditions (BaF_2, BaF_2-air-1d, BaF_2-wet-N_2 and BaF_2-wet-air) corresponding to Lewis acid sites with very weak strength (frequency lower than 2170 cm^{-1}) [6,22,23]. Nevertheless, a decrease of the amount of acid sites was observed when BaF_2 was stored under wet atmosphere (Table 5) illustrated by a significant decrease of the IR band intensities (Fig. 8). Thus, the amount of acid sites was divided by two after only one day of exposure to ambient air (BaF_2-air-1d). This drop was increased in the presence of an atmosphere saturated with water according to the decrease of the surface area. The amount of acid sites was approximately divided by three under wet nitrogen (from 290 to 100 μmol g^{-1}) and by eight under wet air (from 290 to 35 μmol g^{-1}). This decrease corresponded to the sintering of BaF_2 under wet atmosphere (decrease

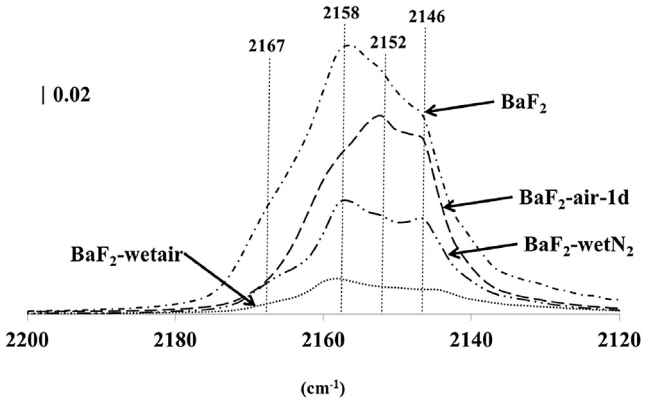

Fig. 8. CO adsorption followed by IR over different BaF_2 samples after activation under HF. Effect of the storage conditions.

Table 5
CO adsorption followed by IR. Amount of acid sites (Q_s per gram and Cs per m^2) of different samples.

Samples	S_{BET} after activation step by HF ($m^2\ g^{-1}$)	Q_s(μmol g^{-1})	C_s(μmol m^{-2})
BaF_2[a]	47	290 (±60)	6.2 (±1.1)
BaF_2-air-1d[a]	42	160 (±30)	3.8 (±0.7)
BaF_2-wet N_2[a]	27	100 (±20)	3.7 (±0.7)
BaF_2-wetair[a]	24	35 (±7)	1.5 (±0.3)
$Ba_{0.5}La_{0.5}F_{2.5}$[a]	38	260 (±50)	6.8 (±1.3)
$Ba_{0.1}La_{0.9}F_{2.9}$[a]	42	200 (±40)	4.8 (±1.0)
LaF_3[a]	75	350 (±70)	4.7 (±1.0)
$BaF_{1.2}Cl_{0.8}$[b]	33	200 (±40)	6.1 (±1.0)

[a] After the activation step by HF.
[b] After 4h30 of transformation of 2-chloropyridine.

of the specific surface area) on the one hand and to the decrease of the concentration of sites per square meter on the other hand. This was particularly significant under wet air (from 6.2 to 1.5 μmol m^{-2}).

The Lewis acidity of mixed $Ba_{0.5}La_{0.5}F_{2.5}$ and $Ba_{0.1}La_{0.9}F_{2.9}$ samples, prepared by precipitation method, after activation by HF was also measured (Fig. 9) and compared to BaF_2 and LaF_3 solids prepared by TDT method. Three bands corresponding to the adsorption of CO on $Ba_{0.5}La_{0.5}F_{2.5}$, $Ba_{0.1}La_{0.9}F_{2.9}$ and LaF_3, respectively at 2165, 2158 and 2151 cm^{-1}, 2167, 2162 and 2154 cm^{-1} and 2178, 2170 and 2164 cm^{-1}, (Fig. 9) were observed. The mixed fluorides possessed intermediate acid strength of sites between BaF_2 and LaF_3. In addition, the higher the lanthanum content, the higher the strength of acidity was. The amount of mixed fluoride Lewis acid sites was relatively close (260 μmol g^{-1} and 200 μmol g^{-1} respectively for $Ba_{0.5}La_{0.5}F_{2.5}$ and $Ba_{0.1}La_{0.9}F_{2.9}$) (Table 5).

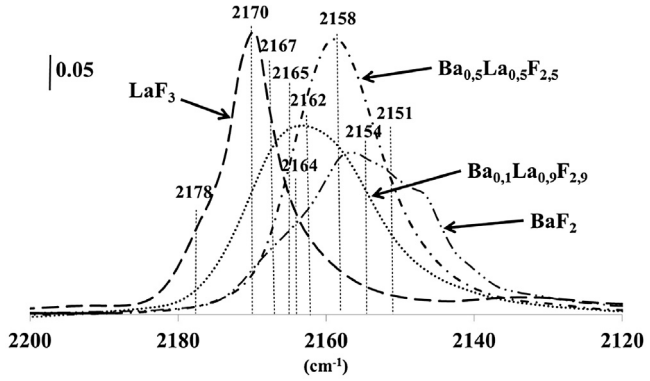

Fig. 9. CO adsorption followed by IR over BaF_2, LaF_3, $Ba_{0.5}La_{0.5}F_{2.5}$ and $Ba_{0.1}La_{0.9}F_{2.9}$ samples. Effect of the presence and the amount of La. For clarity, the bands of BaF_2 are not indexed (see Fig. 8).

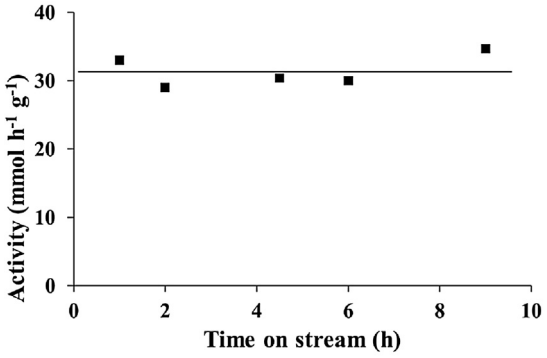

Fig. 10. Transformation of 2-chloropyridine. Activity as a function of time on stream over BaF_2 (T = 300 °C, HF:2-chloropyridine:N_2 = 10.8:1:1.7).

3.4. Transformation of 2-chloropyridine

The impact of the storage atmosphere of BaF_2 and the amount of lanthanum in the Ba-La fluoride systems was measured for the transformation of 2-chloropyridine at 300 °C with a HF/2-chloropyridine ratio of 10.8.

First of all, the establishment of the steady state was fast. Indeed, over BaF_2 (stored in a glove box), the activity for the transformation of 2-chloropyridine measured after different times (from 1 h to 9 h) was constant, around 30 mmol h^{-1} g^{-1} (Fig. 10). XRD, ^{19}F NMR and XPS characterizations showed a chlorination of BaF_2 catalyst, by reaction with the by-product HCl, to a mixed halides of barium which was the real catalyst. BaF_2 changed during the transformation of 2-chloropyridine to the formation of a new crystalline phase, attributed to BaFCl from ICDD database reference files (Fig. 11). The formation of a single phase after transformation of 2-chloropyridine, characterized by a single signal, located at −10.9 ppm, which does not correspond to BaF_2 was confirmed by ^{19}F NMR (Fig. 12). The chlorination of BaF_2 led to a change in the environment of fluorine atom corresponding to an increase in the chemical shift by 4 ppm (-14.9 ppm to −10.9 ppm). In the same way, the presence of chlorine on the catalyst surface was highlighted by XPS (Fig. 13). The composition of the new mixed halides of barium has been determined by titration of barium and fluorine elements (Table 6), the Cl content being determined by difference considering + II as oxidation state for Ba, and by XPS by the quantification of the corresponding peaks (Table 7). The chlorination of BaF_2 was very fast because, the chemical composition of the material ($BaF_{1.4(\pm0.1)}Cl_{0.6}$) was close after 1 h and after 4 h 30 of reaction ($BaF_{1.2(\pm0.1)}Cl_{0.8}$ - Table 6). The composition also corresponded to the elemental one determined by XPS (Table 7). This is consistent

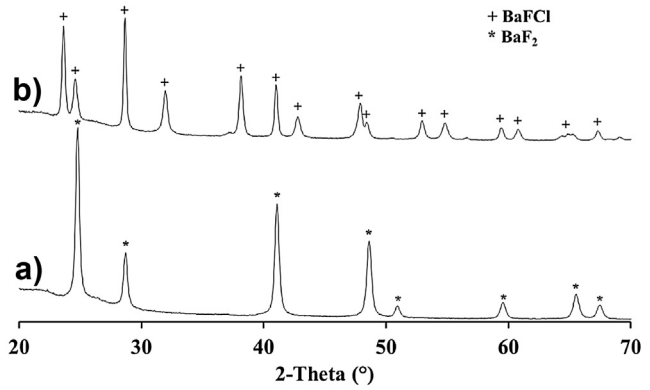

Fig. 11. X-Ray diffraction patter of BaF_2 a) before and b) after the transformation of 2-chloropyridine.

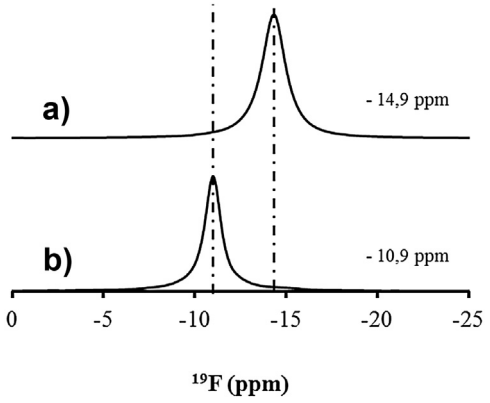

Fig. 12. ^{19}F MAS NMR spectra of BaF_2 a) before and b) after the transformation of 2-chloropyridine.

Table 6
Chemical composition and specific surface area (S_{BET}) of BaF_2 catalysts after the transformation of 2-chloropyridine for different times on stream (T = 300 °C, HF:2-chloropyridine:N_2 = 10.8:1:1.7).

Time on stream (h)	S_{BET} (m^2 g^{-1})	F/Ba molar ratio[a]	Theoretical formula[b]
0	47	2	BaF_2
1	38	1.4(±0.1)	$BaF_{1.4(0.1)}Cl_{0.6(0.1)}$
4h30	33	1.2(±0.1)	$BaF_{1.2(0.1)}Cl_{0.8(0.1)}$

[a] F content was determined by ion chromatography and Ba content by ICP-OES.
[b] The Cl content was determined by difference considering + II as oxidation state for Ba.

Table 7
XPS binding energies and elemental composition of BaF_2 before and after the transformation of 2-chloropyridine (T = 300 °C, 4h30, HF:2-chloropyridine:N_2 = 10.8:1:1.7).

BaF_2	Binding energies (eV)			Molar ratio		
	Ba $3d_{5/2}$	F 1 s	Cl 2p	F/Ba	Cl/Ba	(F+Cl)/Ba
Before reaction	780.2	684.1	–	2.1	0	2.1
After reaction	780.3	684.1	198.7	1.4	0.8	2.2

with the activity which was stable over time on stream (Fig. 10) highlighting no significant modification of the catalyst during the transformation of 2-chloropyridine between 1 and 9 h. Moreover, this chlorination resulted in a very fast and significant decrease of the specific surface of the material (47 to 38 m^2 g^{-1} after 1 h of reaction and to 33 m^2 g^{-1} after 4h30 of reaction). The presence of chlorine atom modified also the Lewis acid properties (Fig. 14). The strength of acidity of $BaF_{1.2}Cl_{0.8}$ obtained after 4h30 of reaction was

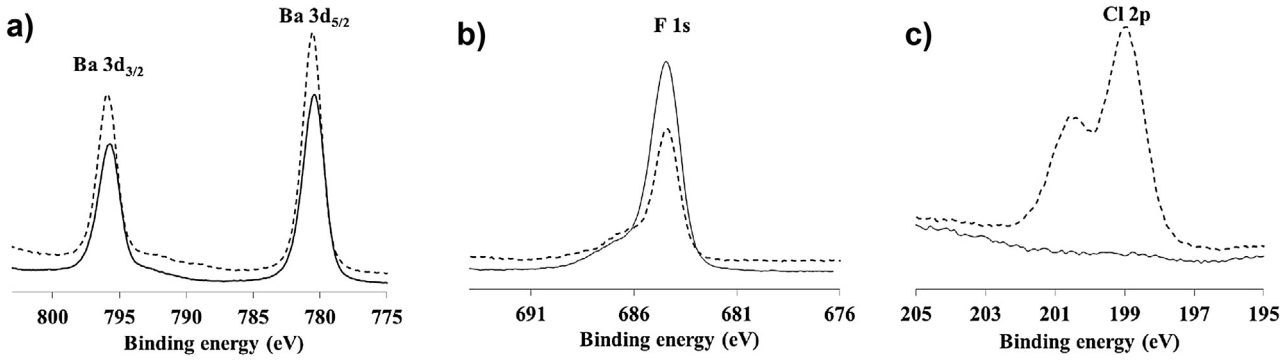

Fig. 13. XPS spectra of barium based catalyst before (solid line) and after the transformation of 2-chloropyridine (dotted line) for a): barium element, b): fluorine element, c): chlorine element.

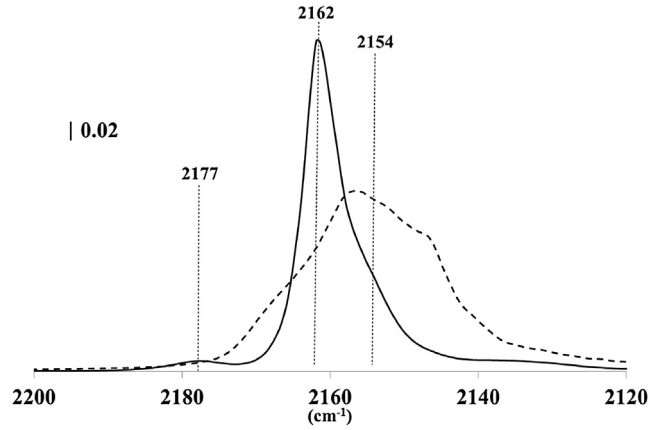

Fig. 14. Adsorption of CO followed by IR. Comparison of BaF_2 (dotted line) and $BaF_{1.2}Cl_{0.8}$ (solid line) formed after transformation of 2-chloropyridine during 4 h 30.

Table 8
Activities for the transformation of 2-chloropyridine (T = 300 °C, 4h30, HF:2-chloropyridine:N_2 = 10.8:1:1.7). Effect of the storage atmosphere of BaF_2.

Samples	S_{BET} after activation step by HF ($m^2\ g^{-1}$)	Activity ($mmol\ h^{-1}\ g^{-1}$)	Activity ($mmol\ h^{-1}\ m^{-2}$)
BaF_2	47	30	0,64
BaF_2-air-1d	42	20	0,47
BaF_2-wet N_2	27	11	0,41
BaF_2-wetair	24	6	0,25

slightly higher than BaF_2. Indeed, the CO adsorption bands were observed at higher wavenumbers (2177, 2162 and 2154 cm^{-1}) than those of BaF_2 (2167, 2158, 2152 and 2146 cm^{-1}). The quantification led to a similar acid site concentration of BaF_2 and $BaF_{1.2}Cl_{0.8}$ (around 6 $\mu mol\ m^{-2}$ -Table 5). The difference of the total amount of Lewis acid sites between both materials (290 $\mu mol\ g^{-1}$ for BaF_2 and 200 $\mu mol\ g^{-1}$ for $BaF_{1.2}Cl_{0.8}$) corresponded only to the decrease of the specific surface area during the chlorination of BaF_2 (47 $m^2\ g^{-1}$ for BaF_2 and 33 $m^2\ g^{-1}$ for $BaF_{1.2}Cl_{0.8}$).

The storage atmosphere of BaF_2 modified strongly the catalytic activity for the transformation of 2-chloropyridine (Table 8). A storage under anhydrous atmosphere retained the catalytic properties of BaF_2 even after 100 days of storage. In contrast, a wet atmosphere storage led to a decrease of the catalytic activity. Indeed, a storage during one day under ambient air was enough to slow down the activity by 33%. This phenomenon was increased under wet atmosphere. Thus, the activity of BaF_2 is divided by three after storage under wetN_2 (30 to 11 $mmol\ h^{-1}\ g^{-1}$) and five under wet air (30 to 6 $mmol\ g^{-1}\ h^{-1}$). The activity per unit square meter also decreases significantly (from 0.64 to 0.25 $mmol\ h^{-1}\ m^{-2}$).

The influence of the introduction of lanthanum into BaF_2 based catalysts from TDT and precipitation methods was studied. The catalytic activities of Ba-La fluorides systems prepared by TDT varied little with La/(Ba + La) molar ratio (from 35 to 41 $mmol\ g^{-1}\ h^{-1}$) (Table 9) and were higher than activities of the monometallic fluorides BaF_2 (30 $mmol\ g^{-1}\ h^{-1}$) and LaF_3 (19 $mmol\ g^{-1}\ h^{-1}$). This gain of activity compared to BaF_2 was mainly due to the increase of the specific surface area of these materials (47 $m^2\ g^{-1}$ for BaF_2 and 63–75 $m^2\ g^{-1}$ for Ba-La fluoride system samples after activation by HF) since the activities per square meter had not evolved very significantly with x (from 0.65 $mmol\ h^{-1}\ m^{-2}$ for x = 0.2 to 0.46 $mmol\ h^{-1}\ m^{-2}$ for x = 0.9). For x = 0.9, the addition of a small amount of barium (only 10 mol%) multiplied by two the catalytic activity per gram and per square meter unit with respect to LaF_3 (35 $mmol\ h^{-1}\ g^{-1}$ or 0.46 $mmol\ h^{-1}\ m^{-2}$ for Ba-La fluoride system with x = 0.9 and 19 $mmol\ h^{-1}\ g^{-1}$ or 0.25 $mmol\ h^{-1}\ m^{-2}$ for LaF_3). The activities of monometallic fluorides (BaF_2, LaF_3) synthesized by precipitation method were much smaller (3 $mmol\ h^{-1}\ g^{-1}$ for BaF_2 and 7 $mmol\ h^{-1}\ g^{-1}$ for LaF_3, Table 9) than those measured for the same compounds prepared by TDT method (30 $mmol\ h^{-1}\ g^{-1}$ for BaF_2 and 19 $mmol\ h^{-1}\ g^{-1}$ for LaF_3). This was mainly based on specific surface areas which were much lower by precipitation method than by TDT method. For $0 \leq x \leq 0.5$, the catalytic activity of samples prepared by precipitation method increased with the La/(La + Ba) molar ratio (x), corresponding to the increase of the amount of active $Ba_{0.5}La_{0.5}F_{2.5}$ mixed phase (44 $mmol\ h^{-1}\ g^{-1}$) relative to the BaF_2 phase which was very small (3 $mmol\ h^{-1}\ g^{-1}$). For $0.5 \leq x \leq 0.9$, the catalytic activity decreased slightly with x, due to the presence of mixed hexagonal phases ($Ba_{0.15}La_{0.85}F_{2.85}$ and $Ba_{0.1}La_{0.9}F_{2.9}$) which were slightly less active (35 $mmol\ h^{-1}\ g^{-1}$ for $Ba_{0.1}La_{0.9}F_{2.9}$) that the cubic phase $Ba_{0.5}La_{0.5}F_{2.5}$ (44 $mmol\ g^{-1}\ h^{-1}$). As the TDT method, a large gain of activity was observed with the addition of a small amount of barium (10 mol%, x = 0.9) in the lanthanum structure. Indeed, the activity per gram of $Ba_{0.1}La_{0.9}F_{2.9}$ was five times higher than LaF_3 (35 $mmol\ h^{-1}\ g^{-1}$ and 7 $mmol\ h^{-1}\ g^{-1}$ respectively) while activity per square meter was three times higher (0.83 $mmol\ h^{-1}\ m^{-2}$ and 0.28 $mmol\ h^{-1}\ m^{-2}$ respectively). Moreover, the formation of mixed fluorides such as $Ba_{0.1}La_{0.9}F_{2.9}$ and $Ba_{0.5}La_{0.5}F_{2.5}$ allowed to avoid the chlorination reaction observed with BaF_2 during the transformation of 2-chloropyridine. Indeed, no structural change was noticed by XRD and no chlorine atom was detected by XPS. Moreover the specific surface area remained stable. From the different catalysts studied on this reaction, the best activity was obtained with $Ba_{0.5}La_{0.5}F_{2.5}$ catalyst.

Table 9
Transformation of 2-chloropyridine. Activity (per gram and m^2) of catalyst with various La/La + Ba (x) molar ratio prepared by TDT and precipitation methods (T = 300 °C, 4h30, HF:2-chloropyridine:N_2 = 10.8:1:1.7).

x	TDT method			Precipitation method		
	S_{BET} (m^2/g)	Activity		S_{BET} ($m^2\ g^{-1}$)	Activity	
		($mmol\ h^{-1}\ g^{-1}$)	($mmol\ h^{-1}\ m^{-2}$)		($mmol\ h^{-1}\ g^{-1}$)	($mmol\ h^{-1}\ m^{-2}$)
0.0	47	30	0.64	<3	3	nd[b]
0.2	63	41	0.65	30	23	0.77
0.33	65	41	0.63	41	37	0.90
0.5	73	41	0.56	38	44	1.16
0.67	71	41	0.58	47	43	0.91
0.8	72	38	0.53	45	42	0.93
0.9	75	35	0.46	42	35	0.83
1.0	75	19	0.25	25	7	0.28

nd: not determined due to the uncertainty on the specific surface area of BaF_2.

4. Discussion

BaF_2, one of the most active catalysts for the transformation of 2-chloropyridine [6] is very sensitive to the storage atmosphere. Short exposure to wet atmosphere alters the microstructural properties of BaF_2, leading to a significant drop of the specific surface area and to an increase of the size of particles. This phenomenon is increased in the presence of atmosphere (air or nitrogen) saturated by water. A mechanism of sintering may be involved by dissolution and recrystallization phenomena as described by Bernache et al. [24] in the literature. A liquid film of BaF_2 dissolved in water (related to moisture of atmosphere) may be formed at the surface of grains promoting the dissolution/diffusion/recrystallization phenomena of BaF_2, characteristic of a sintering process. Sintering is a process which changes a system consisting of individual particles (or porous agglomerates) in the sense of the decrease of the global free energy of this system, leading to a decrease of the porosity and to a growing of particles [24]. Thus, water in the atmosphere acts as a sintering agent for BaF_2. To maintain the properties of BaF_2, it should be stored and handled in a glove box under dry atmosphere. Another way to stabilize the properties of BaF_2 consists to substitute a part of barium by lanthanum in the structure. For this, the preparation of bimetallic fluoride ($Ba_{1-x}La_xF_{2+x}$ with x = La/(La + Ba)) was carried out through TDT and precipitation methods. To our knowledge, $Ba_{1-x}La_xF_{2+x}$ has never been prepared by both methods except for x = 0.43synthesized by co-precipitation [17]. Nevertheless some mixed metal fluorides with M^{2+} and M^{3+} ions has been already obtained by precipitation method such as $Ba_{1-x}Y_xF_{2+x}$, $Ba_{1-x}Sc_xF_{2+x}$, $Ba_{1-x}Ce_xF_{2+x}$ or $Sr_{1-x}Y_xF_{2+x}$ [25–28]. Both methods (TDT and precipitation) do not lead to the same materials. By TDT method, an intimate mixture of BaF_2 and LaF_3 is formed unlike by the precipitation method where mixed phases such as $Ba_{0.5}La_{0.5}F_{2.5}$ and $Ba_{0.1}La_{0.9}F_{2.9}$ crystallize without secondary phase in the same group space corresponding to BaF_2 and LaF_3 respectively. Thus, the introduction of lanthanum into BaF_2 structure and conversely is possible by this method as described by the phase diagram proposed by Sobolev et al. [16]. For $0.5 \leq x \leq 1$, phases obtained by precipitation method correspond to those provided by the phase diagram. In contrast, for $0 < x < 0.5$, a mixture of phases of BaF_2 and $Ba_{0.5}La_{0.5}F_{2.5}$ is obtained when a solid solution $Ba_{1-x}\ La_xF_{2+x}$ is expected. This phenomenon was already observed on the BaF_2-YF_3 system prepared by co-precipitation [28]. Indeed, a mixture of BaF_2 and a fluorite-type $Ba_{1-x}Y_xF_{2+x}$ nanophase was obtained for x lower than 0.35. However, no explanation for this phenomenon was offered. This method allows the formation of $Ba_{1-x}La_xF_{2+x}$ with crystallites lower than 15 nm as determined by Debye-Scherrer equation, these sizes being the smallest reported in the literature (until now: 10–30 nm by mechanosynthesis [11]) and may provide catalysts with higher activity.

The preparation of mixed fluorides or intimate mixtures of BaF_2 and LaF_3 leads to materials with higher specific surface areas than those of the corresponding monometallic fluorides on the one hand, and to a better microstructural stability under wet atmosphere on the other. This stability is total for fluorides prepared by precipitation method, these materials being synthesized in water. From TDT method, the stability is partial, which is due to the presence of BaF_2 in the mixture. Nevertheless, the presence of LaF_3 significantly reduces the decrease of the specific surface area observed for BaF_2 alone. Therefore, a synergistic effect between lanthanum and barium is found between the two metals whatever the method of synthesis and improves the microstructural stability and leads to higher specific surface areas. Moreover, characterization (XPS, NMR, XRD) of BaF_2 after the transformation of 2-chloropyridine show the formation of a single phase $BaF_{1.2}Cl_{0.8}$. This chlorination of BaF_2 by HCl formed during Cl/F exchanges, an exothermic reaction, leads to a decrease of the specific surface area. The presence of lanthanum in the structure ($Ba_{1-x}La_xF_{2+x}$ mixed fluorides) avoids this chlorination and the loss of the specific surface area.

The evolution of the Lewis acidity properties of these materials which were previously identified as a key parameter of the active site (coordinatively unsaturated sites of metal: CUS) for Cl/F exchanges [6] depends on the storage atmosphere and on the presence of lanthanum. The total acidity measured by CO adsorption followed by IR decreases when BaF_2 is stored under wet atmosphere. This is partly due to the decrease of the specific surface area. Nevertheless, more surprising, the concentration per square meter decreases also with the specific surface area (Table 5) whereas the nature of Lewis sites is similar (Fig. 8). This may be explained by the sintering in water leading to an increase of the crystallites size accompanied by the decrease of number of defects (active sites) per square meter such as dislocation or stacking faults. Further investigations with high resolution microscopy should be lead to demonstrate this assumption.

The introduction of lanthanum into BaF_2 structure (for $Ba_{0.5}La_{0.5}F_{2.5}$ and $Ba_{0.1}La_{0.9}F_{2.9}$ compositions) results in a slight increase of the acidity strength in accordance with the electronegativity of lanthanum ($\chi = 1.08$) which is higher than that of barium ($\chi = 0.97$). Nevertheless, although the introduction of lanthanum increases the strength of Lewis acidity, the mixed fluorides ($Ba_{0.5}La_{0.5}F_{2.5}$ and $Ba_{0.1}La_{0.9}F_{2.9}$) retains the behavior of Lewis acidity with very weak strength of BaF_2 since the main ν(CO) bands are lower than 2170 cm^{-1}. In addition, there is a correlation between the concentration of acid sites and the crystalline structure of the materials. Indeed, the concentration of acid sites in BaF_2 and $Ba_{0.5}La_{0.5}F_{2.5}$ with a cubic structure (space group *Fm*-3m) are similar (about 6.5 $\mu mol\ m^{-2}$ – Table 5). This is also checked with LaF_3 and $Ba_{0.1}La_{0.9}F_{2.9}$ with trigonal structure (space group, *P*-3*c*1) which have a concentration of sites of about 4.8 $\mu mol\ m^{-2}$ (Table 5).

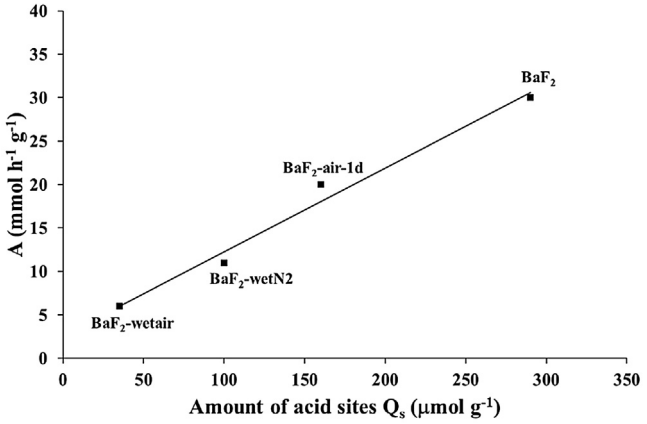

Fig. 15. Transformation of 2-chloropyridine. Effect of the storage atmosphere. Activity as a function of the amount of Lewis acid sites (T = 300 °C, 4h30, HF:2-chloropyridine:N_2 = 10.8:1:1.7).

According to the literature [18], the nature of the acid sites (CUS) is linked to the structural surface of a material. Thus, for catalysts having the same crystallographic structure, the nature of the sites at the catalyst surface may be similar leading to the same concentration of sites per square meter.

On the other hand, the chlorination of BaF_2 by HCl during the transformation of 2-chlorpyridine, allowing the formation of $BaF_{1.2}Cl_{0.8}$, leads to a slight increase of the acidity strength contrary to the results reported in the literature [1]. Indeed, according to this work, the adsorption of CO on BaF_2 and $BaF_{1,3}Cl_{0,7}$ are similar. This change of the Lewis acidity strength is not in accordance with the difference of electronegativity between chlorine and fluorine atoms, fluorine being the most electronegative element. The substitution of fluorine by chlorine atom should induce a decrease of the Lewis acidity strength of the material and not an increase as observed in the present work. This increase can be explained by the change of the crystal structure during the chlorination. Indeed, BaFCl (structure and composition close to $BaF_{1.2}Cl_{0.8}$) is surrounded by more halogen atoms (5 chlorine atoms and 4 fluorine atoms) [29] than BaF_2 (8 fluorine atoms) which decreases the electronic density of the metal and increases its Lewis acidity. Furthermore, the distance between barium and fluorine is shorter for BaFCl than BaF_2, which may favor the higher Lewis acidity [26,30]. Nevertheless, although the strength of Lewis acidity increases with the formation of the mixed halides of barium, Lewis acidity strength remains very weak like in BaF_2 (main ν(CO) bands lower than 2170 cm^{-1} – Fig. 14).

Regarding the catalytic activities of the various barium fluoride catalysts for the transformation of 2-chloropyridine, the storage under wet atmosphere shows a negative impact. Indeed, the activity decreases with the amount of Lewis acid sites as a direct consequence of the sintering of the material. Whatever the atmosphere of storage (wet and dry, nitrogen or air) and the specific surface area, a proportional relationship is established between the catalytic activity and the amount of Lewis acid sites (Fig. 15) which confirms that the same active acid sites are involved in Cl/F exchanges on these different BaF_2. The presence of lanthanum ($Ba_{0.5}La_{0.5}F_{2.5}$ and $Ba_{0.1}La_{0.9}F_{2.9}$ mixed fluorides), which stabilizes the microstructure of BaF_2 against the sintering under wet atmosphere and avoids the chlorination by HCl, leads to higher catalytic activities than $BaF_{1.2}Cl_{0.8}$ which is the real catalyst formed from initial BaF_2 (Table 10). This is mainly due to a gain of specific surface area, the TOF (Turn Over Frequency defined as the ratio between the catalytic activity and the number of active sites determined by CO adsorption followed by IR) of these three materials being very close (between 155 and 175 h^{-1}). Interestingly, the introduction of only 10 mol% of barium in the lanthanum structure ($Ba_{0.1}La_{0.9}F_{2.9}$) multiplies the TOF by three (55 h^{-1} for LaF_3 and 175 h^{-1} for $Ba_{0.1}La_{0.9}F_{2.9}$) while the strength of Lewis acidity is fairly similar for both catalysts (Fig. 9). This confirms that other parameters than the strength of acidity are involved in the Cl/F exchange reaction in the presence of barium, the most active element [6]. The higher activity may result from the special affinity between the barium atom and the chlorine atom as already shown in the literature [1,31]. In this case, we proposed that 2-chloropyridine may be adsorbed not only by nitrogen atom as described previously [6] but also by chlorine atom. The adsorption by the chlorine atom would result in an activation of the C—Cl bond which then promotes Cl/F exchange.

Table 10
Transformation of 2-chloropyridine. Amount of acid sites (Q_s), activities (A) and Turn Over Frequencies (TOF) of different catalysts (T = 300 °C, 4h30, HF:2-chloropyridine:N_2 = 10.8:1:1.7).

Catalyst	Q_s[a] (µmol g^{-1})	A (mmol h^{-1} g^{-1})	TOF (h^{-1})
$BaF_{1.2}Cl_{0.8}$	200 (±40)	31	155 (±20)
$Ba_{0.5}La_{0.5}F_{2.5}$	260 (±50)	44	170 (±20)
$Ba_{0.1}La_{0.9}F_{2.9}$	200 (±40)	35	175 (±20)
LaF_3	350 (±70)	19	55 (±15)

5. Conclusion

In this work, BaF_2-LaF_3 system was explored as a catalyst for the fluorination of 2-chloropyridine by Cl/F exchange with HF as fluorinating agent.

Thermal decomposition of metal trifluoroacetates (TDT) and precipitation were explored as synthesis methods. Depending on the synthesis method, an intimate mixture of monometallic fluorides, BaF_2 and LaF_3 (by TDT) or a mixture of $Ba_{1-x}La_xF_{2+x}$ mixed fluorides (by precipitation method) were obtained. Moreover, pure single mixed fluorides with x = 0.5 (with a fluorite structure) and 0.9 (with a tysonite structure) were synthesized for the first time by precipitation method. These materials were synthesized with significant specific surface areas (mainly between 50 and 150 m^2 g^{-1}) and small crystallite sizes (5–15 nm). A synergetic effect between the lanthanum and the barium was highlighted since the preparation of a mixture of BaF_2 and LaF_3 by TDT led to higher specific surface area (84–100 m^2 g^{-1}) than the corresponding monometallic fluorides (63 and 81 m^2 g^{-1}). In order to obtain high specific surface area, the TDT method is more adapted for the monometallic fluorides than the precipitation method. Nevertheless, only the precipitation method led to pure mixed fluorides in this work. Moreover, the precipitation method, which is a method widely used to prepare solid catalysts in industry, is simpler, environmentally friendly, cheaper and easier to scale up than the TDT method.

Moreover, mixed barium-lanthanum fluorides ($Ba_{0.5}La_{0.5}F_{2.5}$ and $Ba_{0.1}La_{0.9}F_{2.9}$) synthesized by precipitation method are the most active catalyst for the transformation of 2-chloropyridine. These materials are stable regarding wet atmosphere, contrary to BaF_2, allowing the storage of the mixed materials without any precaution. Indeed, water has been identified as a sintering agent which explains the decrease of the specific surface area corresponding to an increase of the size of particles of BaF_2. Moreover, the presence of lanthanum avoids the chlorination of the catalyst observed on BaF_2 during the transformation of 2-chloropyridine. Thus, thanks to their properties, $Ba_{1-x}La_xF_{2+x}$ mixed fluorides are promising catalysts for this reaction, and beyond, for reactions involving solid catalysts with weak strength of Lewis acidity.

Acknowledgments

A. Astruc thanks CNRS for a PhD grant. The authors would like to thank Stéphane Pronier for TEM characterization.

This work was funded by the French ANR Programme National de Recherche – FLUORCAT, a joint project between the Centre National de la Recherche Scientifique (CNRS), the universities of Lille and Poitiers and Solvay. We acknowledge The *Fonds Européen de Développement Régional* (FEDER), *CNRS*, *Région Nord Pas-de-Calais* and *Ministère de l'Education Nationale de l'Enseignement Supérieur et de la Recherche* for fundings of XPS/LEIS/ToF-SIMS spectrometers within the *Pôle Régional d'Analyses de Surface*. Financial support from the IR RMN THC Fr3050 for conducting the research is also gratefully acknowledged.

References

[1] K. Teinz, S. Wuttke, F. Börno, J. Eicher, E. Kemnitz, J. Catal. 282 (2011) 175–182.
[2] H.X. Dai, Y.W. Liu, C.F. Ng, C.T. Au, J. Catal. 187 (1999) 59–76.
[3] C.-T. Au, X. Zhou, J. Chem. Soc. Faraday Trans. 93 (1997) 485–549.
[4] C.T. Au, H. He, S.Y. Lai, C.F. Ng, J. Catal. 159 (1996) 280–287.
[5] R. Long, J. Luo, M. Chen, H. Wan, Appl. Catal. A: Gen. 159 (1997) 171–185.
[6] A. Astruc, C. Cochon, S. Dessources, S. Célérier, S. Brunet, Appl. Catal. A: Gen. 453 (2013) 20–27.
[7] C. Cochon, S. Célérier, A. Riviere, K. Vigier, J.-D. Comparot, F. Metz, S. Brunet, Catal. Commun. 12 (2010) 151–153.
[8] C. Cochon, T. Corre, S. Célérier, S. Brunet, Appl. Catal. A: Gen. 413–414 (2012) 149–156.
[9] J. Chable, B. Dieudonné, M. Body, C. Legein, M.-P. Crosnier-Lopez, C. Galven, F. Mauvy, E. Durand, S. Fourcade, D. Sheptyakov, M. Leblanc, V. Maisonneuve, A. Demourgues, Dalton Trans. 44 (2015) 19625–19635.
[10] C. Rongeat, M. Anji Reddy, R. Witter, M. Fichtner, J. Phys. Chem. C 117 (2013) 4943–4950.
[11] A. Duvel, J. Bednarcik, V. Sepelak, P. Heitjans, J. Phys. Chem. C 118 (2014) 7117–7129.
[12] N.I. Sorokin, B.P. Sobolev, Crystallogr. Rep. 52 (2007) 842–863.
[13] K.S. Gavrichev, A.V. Tyurin, A.V. Khoroshilov, M.A. Ryumin, V.M. Gurevich, P.P. Fedorov, Thermochim. Acta 558 (2013) 1–5.
[14] L.-P. Jia, Q. Zhang, B. Yan, Mater. Res. Bull. 55 (2014) 53–60.
[15] J.T. Stecher, A.B. Rohlfing, M.J. Therien, Nanomaterials 4 (2014) 69–86.
[16] B.P. Sobolev, N.L. Tkachenko, J. Less-Common Met. 85 (1982) 155–170.
[17] S.V. Kuznetsov, P.P. Fedorov, V.V. Voronov, K.S. Samarina, R.P. Ermakov, V.V. Osiko, Russ. J. Inorg. Chem. 55 (2010) 484–493.
[18] S. Wuttke, A. Vimont, J.-C. Lavalley, M. Daturi, E. Kemnitz, J. Phys. Chem. C 114 (2010) 5113–5120.
[19] S.Y. Arkhipenko, A.A. Fedorova, I.V. Morozov, A.S. Shaporev, Mendeleev Commun. 22 (2012) 25–26.
[20] T.Y. Glazunova, A.I. Boltalin, P.P. Fedorov, Russ. J. Inorg. Chem. 51 (2006) 983–987.
[21] A. Sadoc, M. Body, C. Legein, M. Biswal, F. Fayon, X. Rocquefelte, F. Boucher, Phys. Chem. Chem. Phys. 13 (2011) 18539–18550.
[22] T. Krahl, A. Vimont, G. Eltanany, M. Daturi, E. Kemnitz, J. Phys. Chem. C 111 (2007) 18317–18325.
[23] S. Wuttke, S.M. Coman, G. Scholz, H. Kirmse, A. Vimont, M. Daturi, S.L.M. Schroeder, E. Kemnitz, J. Chem. Eur. 14 (2008) 11488–11499.
[24] D. Bernache-Assolant, Chimie-physique du frittage, Forceram Hermès, 1993.
[25] M.N. Mayakova, S.V. Kuznetsov, P.P. Fedorov, V.V. Voronov, R.P. Ermakov, K.N. Boldyrev, O.V. Karban, O.V. Uravov, A.E. Baranchikov, V.V. Osiko, Inorg. Mater. 49 (2013) 1152–1156.
[26] M.N. Mayakova, V.V. Voronov, L.D. Iskhakova, S.V. Kuznetsov, P.P. Fedorov, J. Fluorine Chem. 187 (2016) 33–39.
[27] M.N. Mayakova, S.V. Kuznetsov, V.V. Voronov, A.E. Baranchikov, V.K. Ivanov, P.P. Fedorov, Russ. J. Inorg. Chem. 59 (2014) 773–777.
[28] P.P. Fedorov, M.N. Mayakova, S.V. Kuznetsov, V.V. Voronov, R.P. Ermakov, K.S. Samarina, A.I. Popov, V.V. Osiko, Mater. Res. Bull. 47 (2012) 1794–1799.
[29] M. Sieskind, J. Morel, J. Solid State Chem. 144 (1999) 339–348.
[30] G.E. Brown, A.S. Radtke, Golden Book of Phase Transitions, Wroclaw, 2002, pp. 1–123.
[31] K. Teinz, S. Manuel, B. Chen, A. Pigamo, N. Doucet, E. Kemnitz, Appl. Catal. B: Environ. 165 (2015) 200–208.